Muon $g-2$, Dark Matter, and Lepton Flavor Violation in SUSY-GUT's

Mario E. Gómez,[1] Smaragda Lola,[2] Qaisar Shafi,[3] Amit Tiwari,[3] and Cem Salih Ün[1,4]

[1]*Departamento de Ciencias Integradas y Centro de Estudios Avanzados en Física Matemáticas y Computación, Campus El Carmen, Universidad de Huelva, 21071 Huelva, Spain*

[2]*Department of Physics, University of Patras, 26500 Patras, Greece*

[3]*Department of Physics and Astronomy, University of Delaware, Newark, DE 19716, USA*

[4]*Department of Physics, Bursa Uludağ University, TR16059 Bursa, Turkey*

Abstract

We perform an analysis of the predictions of several supersymmetric Grand Unified Theories (GUTs) for Dark Matter and the measurements of the muon anomalous magnetic moment (muon $g-2$) consistent with possible Lepton Flavor Violating (LFV) signal in charged lepton decays. Each GUT predicts different Dark Matter (DM) scenarios, which can be used to classify SUSY models and contrast their predictions with experimental evidences. We find that models arising from $SU(4)_c \times SU(2)_L \times SU(2)_R$ can predict DM of cosmological interest while explaining the observed value of the muon $g-2$. Furthermore, we show that when this framework is extended with a simple type 1 seesaw mechanism to explain neutrino masses, many models also predict charged LFV decays that can be observed in current experiments.

Keywords: supersymmetry, phenomenology
DOI: 10.31526/LHEP.2023.381

1. INTRODUCTION

Despite the success of the Standard Model (SM), it cannot be considered the definitive theory of fundamental interactions. For instance, it cannot explain some of the top problems in the current Particle Physics, such as the observed neutrino flavor oscillations, and also cannot provide a suitable Dark Matter (DM) candidate to explain its cosmological evidence [1, 3]. Moreover, theoretical issues, such as the hierarchy problem and unification of the fundamental interactions, have motivated searches for fundamental theories in which the SM arises as a low energy approximation. In particular, Supersymmetric (SUSY) extensions of the SM [5] predict the unification of the three fundamental SM interactions at a high energy scale called $M_{\rm GUT}$. At this scale, it is possible to postulate [6, 7, 8] that the $SU(3)_c \times SU(2)_L \times U(1)_Y$ arises after the breaking of a higher symmetry that unifies the three interactions and it is operative from $M_{\rm GUT}$ to a scale M_X where gravity also unifies with the other interactions.

SUSY contributions to phenomena predicted by the SM can also provide a solution to discrepancies between SM theoretical values and their experimental measurements. This is the case of the BR$(b \to s\gamma)$ [9] and the value of the muon anomalous magnetic moment (hereafter muon $g-2$) [10, 11, 12]. Regarding the latter, Fermilab has recently provided a new experimental value for muon $g-2$, which deviates from the SM prediction by 3.3σ [13]. By combining this discrepancy with the previous measurements at the Brookhaven National Laboratory [14], the following world average in the muon $g-2$ measurements is obtained:

$$\Delta a_\mu \equiv a_\mu^{\rm exp} - a_\mu^{\rm SM} = (25.1 \pm 5.9) \times 10^{-10}. \tag{1}$$

This new world average points to a 4.2σ deviation from the SM predictions [15, 16, 17].

Besides the contribution to the SM processes, SUSY can also explain rare processes forbidden by the SM and therefore, which can be considered a signal for new physics. Among those, the violation of the leptonic flavor (LFV) is one of the most interesting problems from both theoretical and experimental points of view [18]. The current bounds on LFV rare decays of leptons [19] are very restrictive:

$$\begin{aligned} {\rm BR}(\mu \to e\gamma) &< 5.6 \times 10^{-13}, \\ {\rm BR}(\tau \to \mu\gamma) &< 4.4 \times 10^{-8}, \\ {\rm BR}(\tau \to e\gamma) &< 3.3 \times 10^{-8}. \end{aligned} \tag{2}$$

However, they are very interesting from the theoretical point of view since they can be associated with the observed neutrino flavor oscillations [20, 21, 22, 23, 24, 25]. Moreover, these decays can be also correlated with muon $g-2$ problem since their computation involves the same kind of particles and interactions as those in the SUSY contribution to the muon $g-2$ [26].

In this presentation, we will compare several GUT scenarios. Predictions from GUT's preserving the discrete LR symmetry on the soft SUSY-breaking terms (SSB) such as $SO(10)$ or $SU(4)_c \times SU(2)_L \times SU(2)_R$ (4-2-2 for short) presented in [29, 30] are confronted with the LR violating the 4-2-2 framework of [27]. We find that in the 4-2-2 scenario it is possible to find models that can explain the muon $g-2$ problem at the same time as providing good DM candidates. Furthermore, we

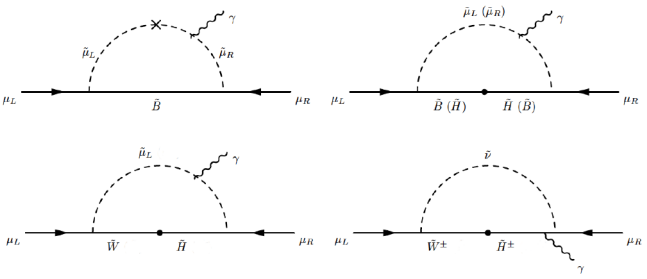

FIGURE 1: The leading contributions to the muon $g-2$ through neutralino and chargino loops. The cross in the top-left diagram denotes the chirality flip between the left- and right-handed smuons, while the dots in the other diagrams represent the mixing between different Neutralino species. In the top-right diagram, there is another loop which is formed by the particles given in parentheses.

discuss that by extending the model with the simple seesaw mechanism used in [29, 30], it is possible to study the LFV predictions of models that solve simultaneously the problems of the DM and the muon $g-2$. The presentation is organized as follows: we discuss the SUSY contribution to muon $g-2$ in Section 2, the relation between the GUT models and the DM candidates in Section 3, and the predictions of the model presented in [27] in Sections 4 and 5 and leave the last section for conclusions.

2. SUSY CONTRIBUTION TO MUON $g-2$

The SUSY contribution to the muon $g-2$ at one loop arises from the diagrams in Figure 1. The upper left one is responsible for the dominant contribution to muon $g-2$ that can be approximately computed by the expression [31]:

$$\Delta a_\mu^{\tilde{B}\tilde{\mu}_L\tilde{\mu}_R} \simeq \frac{g_1^2}{16\pi^2}\frac{m_\mu^2 M_{\tilde{B}}\left(\mu\tan\beta - A_\mu\right)}{m_{\tilde{\mu}_L}^2 m_{\tilde{\mu}_R}^2} F_N\left(\frac{m_{\tilde{\mu}_L}^2}{M_{\tilde{B}}^2}, \frac{m_{\tilde{\mu}_R}^2}{M_{\tilde{B}}^2}\right), \quad (3)$$

where

$$F_N(x,y) = xy\left[\frac{-3+x+y+xy}{(x-1)^2(y-1)^2} + \frac{2x\log(x)}{(x-y)(x-1)^3} - \frac{2y\log(y)}{(x-y)(y-1)^3}\right]. \quad (4)$$

The remaining diagrams in Figure 1 are suppressed by the small Yukawa couplings of the lighter generations. The SUSY contribution to the muon $g-2$ decreases as the SUSY spectrum gets heavier. Therefore, it can account for the discrepancy when the masses of the SUSY particles are relatively small. In contrast, the main SUSY contributions to the Higgs boson mass [32] are

$$\Delta m_h^2 \simeq \frac{m_t^4}{16\pi^2 v^2 \sin^2\beta}\frac{\mu A_t}{M_{\rm SUSY}^2}\left[\frac{A_t^2}{M_{\rm SUSY}^2} - 6\right] + \frac{y_b^4 v^2}{16\pi^2}\sin^2\beta\frac{\mu^3 A_b}{M_{\rm SUSY}^4} + \frac{y_\tau^4 v^2}{48\pi^2}\sin^2\beta\frac{\mu^3 A_\tau}{m_{\tilde{\tau}}^4}, \quad (5)$$

where $M_{\rm SUSY} \equiv \sqrt{m_{\tilde{t}_L} m_{\tilde{t}_R}}$. The above contribution requires relatively large squark masses to accommodate a Higgs boson mass of about 125 GeV while equation (4) shows that the SUSY contribution to muon $g-2$ is enhanced with light sleptons. Therefore, there is a tension between the desired muon $g-2$ contributions and the measured SM-like Higgs boson mass. In some extensions of the SM, D-term contributions to the Higgs boson mass can improve the situation [33]. However, in SUSY models with flavor blind soft terms, this tension is difficult to be relaxed since a correct prediction of the Higgs boson mass requires large 3rd generation squarks while the muon $g-2$ can be solved for low 2nd generation sfermion masses. However, when the MSSM is embedded into a GUT, symmetries of the unification group can impose relations among the soft terms that may relax this tension. For instance, we can assume that the soft masses assigned to SUSY partners of fields depend on the representation of the group to which they belong [38, 39, 40]. Moreover, the conditions imposed by the symmetry on the gauge unification may also relax the gaugino mass unification at the GUT scale. Therefore, the GUT splitting of the gaugino mass is translated by the renormalization group equations (RGEs) to a further splitting among squarks and sfermion that may also help to solve the tension between the two contributions. In the next section, we present two examples of these GUTs [28]: a minimal $SO(10)$ where we consider nonuniversal soft masses for the Higgses mass terms at the GUT scale and a 4-2-2 model where in addition to those the gaugino mass unification is released.

3. GUT MASS RELATIONS AND DM CANDIDATES

Theories that combine supersymmetry with a unification symmetry group for the fundamental interactions (GUTs) require the breaking of the two symmetries. SUSY can be broken by a mechanism that generates flavor blind soft masses to the superpartners at an energy scale M_X, while the GUT group is broken to the SM symmetry at a lower scale $M_{\rm GUT}$. Between the two scales, renormalization can induce flavor dependence on the soft terms. However, since the GUT symmetry is still active, particles belonging to the same representation still have common soft masses at $M_{\rm GUT}$. In terms of a common soft mass m_0 for scalars, we assume that at $M_{\rm GUT}$ particles belonging to a representation r have this mass modified by a factor x_r. This factor accounts for the renormalization effects from M_X to

$M_{\rm GUT}$ and other possible contributions from the specific pattern of the symmetry breaking of the GUT symmetry or additional flavor symmetries. Therefore,

$$m_r = x_r m_0, \tag{6}$$

while the trilinear terms are defined as

$$A_r = Y_r A_0, \quad A_0 = a_0 m_0. \tag{7}$$

Here, Y_r is the Yukawa coupling associated with the r representation. We use the standard parametrization, with a_0 being a dimensionless factor, which we consider as representation independent.

In this section, we will apply the idea presented above to two simple symmetry groups, where the symmetry can be used to explain non universality either on the scalar masses ($SO(10)$) or on the gaugino mass terms (4-2-2) [28].

(i) $SO(10)$

A simple unification scheme arises within an $SO(10)$ GUT, in which all quarks and leptons are accommodated in the same **16** dimensional representation, leading to left-right symmetric mass matrices. We do not consider any particular pattern for the breaking of the GUT symmetry; we just assume that the up and down MSSM Higgs bosons are in a pair of **10**-dimensional representations. This assignment determines sfermion mass matrices and beta functions and results in a common mass for all sfermions and two different Higgs masses m_{h_u} and m_{h_d}. Therefore, in addition to the universal SSB parameters of models like the Constrained MSSM (CMSSM), we introduce two new parameters, x_u and x_d, defined as

$$m_{16} = m_0, \quad m_{H_u} = x_u m_{16}, \quad m_{H_d} = x_d m_{16}. \tag{8}$$

Similarly, the A-terms are defined as

$$A_{16} = a_0 \cdot m_0. \tag{9}$$

(ii) 4-2-2

Here, we will focus on a left-right symmetric 4-2-2 model [34, 35] that will be called symmetric LR 4-2-2 or sLR 4-2-2, leaving the discussion of a more general case, without LR symmetry (aLR 4-2-2), for the next section. We use this simplified model to reduce the number of free parameters such that its results can be more directly compared with the ones of $SO(10)$. In this case, the gaugino masses associated with $SU(2)_L$ and $SU(2)_R$ are the same, while the gluino mass, associated with $SU(4)_c$, can be different.

The relations among soft terms are the following:

(i) Gaugino masses: the hypercharge generator from 4-2-2 implies the relation

$$M_1 = \frac{3}{5} M_2 + \frac{2}{5} M_3. \tag{10}$$

(ii) Soft masses: all sfermions are accommodated in a 16-representation and have a common mass $m_{16} = m_0$. The Higgs fields are in a 10-dimensional representation with D-term contributions that result to $m^2_{H_{u,d}} = m^2_{10} \pm 2M^2_D$. In our notation, these values are

$$r_u = \frac{m_{H_u}}{m_{16}}, \qquad r_u = \frac{m_{H_d}}{m_{16}}, \tag{11}$$

with $r_u < r_d$.

In our computations, we assume a common unification scale $M_{\rm GUT}$ defined as the meeting point of the g_1 and g_2 gauge couplings. The GUT value for g_3 is obtained by requiring $\alpha_s(M_Z) = 0.118$. Above $M_{\rm GUT}$, we assume a unification group that breaks at this scale. We perform a parameter space scan using, as a guide, the representation pattern at the GUT scale for soft scalar terms. For this purpose, we extend the CMSSM universal scenario through nonunified soft terms, consistent with the representations of $SO(10)$ and 4-2-2.

The GUT mass relations can lead to different SUSY mass spectra, depending on the unification group. These relations determine the composition of the LSP and also the nature of the NLSP, since the relic density constraint [3]

$$\Omega_\chi h^2 = 0.1186 \pm 0.0031 \tag{12}$$

imposes strong conditions on the DM candidate. These conditions can be used to classify the different LSPs in models that can satisfy this bound. For instance, in the MSSM, the most common mechanisms to satisfy the relic density condition are as follows.

(i) **Higgsino DM:** $h_f > 0.1$, $|m_A - 2m_\chi| > 0.1 m_\chi$. Here, the parameter h_f is the Higgsino fraction of the lightest neutralino mass eigenstate defined as $h_f \equiv |N_{13}|^2 + |N_{14}|^2$, where N_{ij} are the elements of the unitary mixing matrix that correspond to the Higgsino mass states.

(ii) $\tilde{\tau} - \chi$ **coannihilations:** $h_f < 0.1$, $(m_{\tilde{\tau}_1} - m_\chi) \leq 0.1 m_\chi$.

(iii) A/H **resonances:** $|m_A - 2m_\chi| \leq 0.1 m_\chi$.

The relation of parameters imposed by $SU(5)$ allows further coannihilation mechanisms:

- $\tilde{\tau} - \tilde{\nu}_\tau - \chi$ **coannihilations:** $h_f < 0.1$, $(m_{\tilde{\tau}_1} - m_\chi) \leq 0.1 m_\chi$, $(m_{\tilde{\nu}_\tau} - m_\chi) \leq 0.1 m_\chi$.

The sLR 4-2-2 model introduces a relation among gaugino masses and LR asymmetry that leads to new kinds of coannihilations:

(i) $\tilde{\chi}^+ - \chi$ **coannihilations:** $h_f < 0.1$, $(m_{\tilde{\chi}^+} - m_\chi) \leq 0.1 m_\chi$. In this case, the Higgsino component in the LSP is small, but the lightest chargino is light and nearly degenerates with the bino-like neutralino.

(ii) $\tilde{g} - \chi$ **coannihilations:** $h_f < 0.1$, $(m_{\tilde{g}} - m_\chi) \leq 0.1 m_\chi$. In this case, the gluino can be relatively light and nearly degenerate with the bino-like neutralino.

(iii) $\tilde{t}_1 - \chi$ **coannihilations:** $h_f < 0.1$, $(m_{\tilde{t}_1} - m_\chi) \leq 0.1 m_\chi$. Small values of M_3 can contribute to decreasing the stop masses, thus allowing stop coannihilations.

To produce Figures 2 and 3, we perform runs with soft terms up to 10 TeV and a parameter range summarized as follows:

$$\begin{aligned} 100\,\text{GeV} \leq m_0 \leq 10\,\text{TeV}, \\ 50\,\text{GeV} \leq M_1 \leq 4\,\text{TeV}, \\ 50\,\text{GeV} \leq M_2 \leq 4\,\text{TeV}, \\ -10\,\text{TeV} \leq A_0 \leq 10\,\text{TeV}, \\ 2 \leq \tan\beta \leq 65, \\ -1.9 \leq x_u \leq 1.5, \\ 0 \leq x_d \leq 3.4, \\ x_u \leq x_d. \end{aligned} \tag{13}$$

In the case of $SO(10)$, we consider $M_1 = M_2 = M_3$, while in the sLR 4-2-2 scenario, the relation in equation (10) is assumed. For our analysis, we use the search method described in [28] to select SUSY models that satisfy the bounds listed as follows:

$$\begin{aligned} m_{h_l} = 123\text{–}127\,\text{GeV}, \\ m_{\tilde{g}} \geq 2.1\,\text{TeV}\ (800\,\text{GeV if it is NLSP}), \\ 0.8 \times 10^{-9} \leq \text{BR}\left(B_s \to \mu^+\mu^-\right) \leq 6.2 \times 10^{-9}\,(2\sigma), \\ 2.99 \times 10^{-4} \leq \text{BR}\left(B \to X_s\gamma\right) \leq 3.87 \times 10^{-4}\,(2\sigma), \\ 0.114 \leq \Omega_{\text{CDM}} h^2 \leq 0.126. \end{aligned} \tag{14}$$

In Figures 2 and 3, we can see that a few models can solve the $g-2$ problem but only within $3-\sigma$. In the case of $SO(10)$, these models present $\tilde{\tau} - \chi$ coannihilations while in the sLR 4-2-2 framework also models with $\tilde{\chi}^+ - \chi$ coanihilations can enter in the region. Despite the fact that the $2-\sigma$ level for the muon $g-2$ is not reached in any model, the sLR 4-2-2 case shows a larger contribution to the muon $g-2$. This can be attributed to the fact that 4-2-2 GUT allows larger values for M_3 than the $SO(10)$. Consequently, the mass difference between leptons and stops induced by the RGEs is larger in the sLR 4-2-2 cases, and therefore, the tension between the muon $g-2$ and the correct prediction to the Higgs boson mass is ameliorated.

Figures 4 and 5 present the gluino mass versus the LSP mass predicted in the $SO(10)$ and the sLR 4-2-2 scenarios, respectively. The red line represents the combined line obtained with the LHC bounds based in simple models [36]; it can be considered an indication on the range of parameters that can be explored by the LHC. We can see that models in sLR 4-2-2 scenario present larger gluino masses due to the fact of allowing

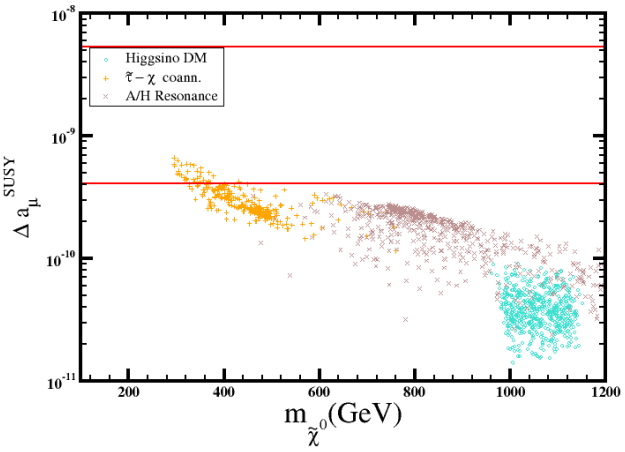

FIGURE 2: Prediction for muon $g-2$ versus m_χ in S0(10) framework. The red lines denote the $3-\sigma$ bounds for the experimental discrepancy of Δa_μ with respect to the SM prediction. Different symbols and color codes are assigned to each class of models, and this notation is maintained in the rest of the plots: Turquoise dots stand for Higgsino DM, brown crosses for A/H resonances, and orange plus for $\tilde{\tau} - \chi$ coannihilations.

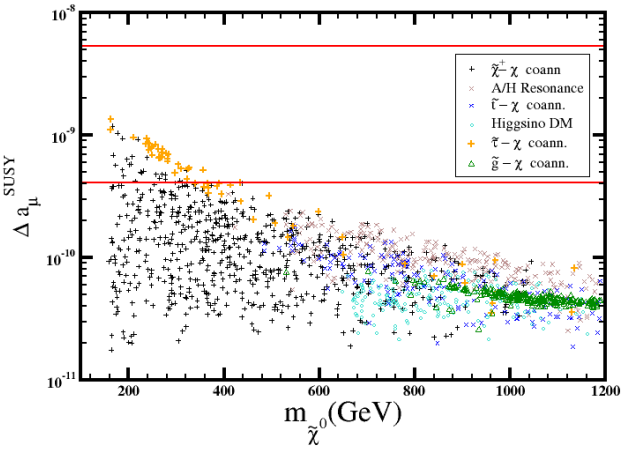

FIGURE 3: Prediction for muon $g-2$ versus m_χ in sLR 4-2-2 framework. The red lines denote the $3-\sigma$ bounds for the experimental discrepancy of Δa_μ with respect to the SM prediction. Different symbols and color codes are assigned to each class of models, and this notation is maintained in the rest of the plots: Turquoise dots stand for Higgsino DM, black plus for $\chi^\pm - \chi$ coannihilations, brown crosses for A/H resonances, blue crosses for $\tilde{t} - \chi$ coannihilations, orange plus for $\tilde{\tau} - \chi$ coannihilations, and green triangles for $\tilde{g} - \chi$ coannihilations.

a GUT splitting on gaugino masses. The same reason explains the possibility of models with gauginos as the NLSP. As we explain before, large gluino masses favor the fitting of the muon $g-2$ observations in SUSY models; however, the preservation of LR symmetry in the presented sLR 4-2-2 scenario equation

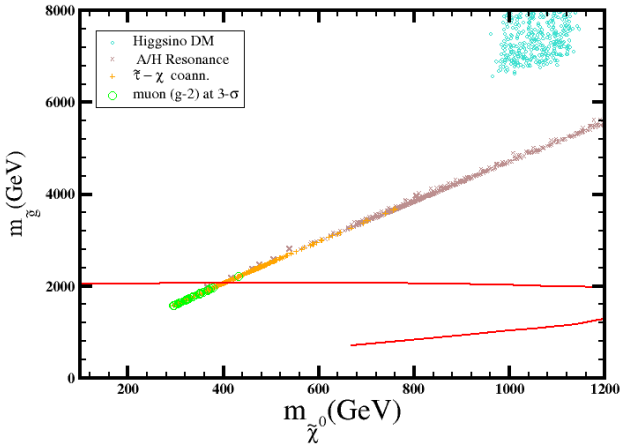

FIGURE 4: Plane $m_{\tilde{g}} - m_{\chi}$ for the $SO(10)$ scenario. The colors represent the same models as in Figure 2. We denote now in green the models compatible with the muon $g-2$ measurements within $3-\sigma$. The red line set the bounds of the parameter space at the reach of the LHC [36].

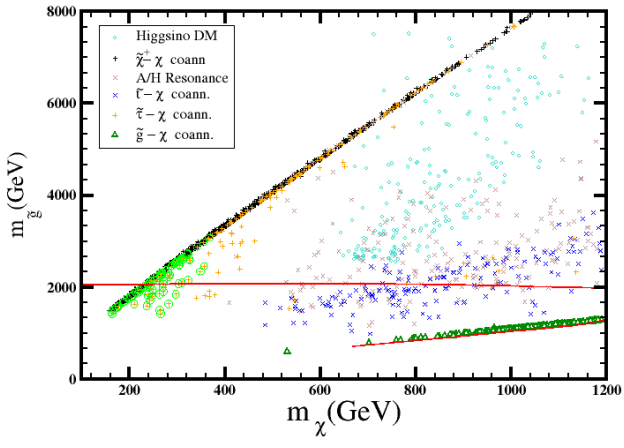

FIGURE 5: Plane $m_{\tilde{g}} - m_{\chi}$ for the sLR 4-2-2 scenario. The colors represent the same models as in Figures 3 and 4.

(16) does not allow very large values for gluino masses while keeping the masses of bino and wino below the TeV scale. In the next section, we will analyze the effect of the breaking of the LR symmetry in a scenario with a different realization of the 4-2-2 symmetry.

4. MUON $g-2$ IN A 4-2-2 MODEL WITHOUT LR SYMMETRY AND HEAVY GAUGINOS

We have shown in the previous section that by relaxing the gaugino mass unification condition at the GUT scale it is possible to increase the size of the SUSY contribution to the muon $(g-2)$. In this section, we will introduce another possible realization of the 4-2-2 symmetry allowing models that can conciliate the theoretical prediction and the experimental findings within $1-\sigma$. This scenario [37] allows larger gaugino masses and also breaks the LR symmetry at the GUT level. In order to distinguish it from the sLR 4-2-2 presented in the previous section, we will refer to it as the aLR 4-2-2.

In the case of the aLR 4-2-2, the breaking of 4-2-2 to the MSSM gauge group leaves intact the hypercharge generator Y, where

$$Y = \sqrt{\frac{3}{5}} I_{3R} + \sqrt{\frac{2}{5}}(B-L), \tag{15}$$

where I_{3R} and $B-L$ represent the diagonal generators of $SU(2)_R$ and $SU(4)_c$, respectively. Consequently, we can assume a relation among the three SSB gaugino masses at the GUT scale given by

$$M_1 = \frac{3}{5} M_{2R} + \frac{2}{5} M_4, \tag{16}$$

where M_{2R} and M_4 denote the gaugino mass terms for $SU(2)_R$ and $SU(4)_c$, respectively, and $M_3 = M_4$ at $M_{\rm GUT}$. In this model, the LR breaking in the gaugino sector can be parametrized as $M_{2R} = y_{LR} M_{2L}$, where $M_{2L} = M_2$ is the SSB mass of $SU(2)_L$ gaugino. These relations allow values for M_3 much larger than the models in the previous section. Therefore, the nonuniversality of the gaugino masses helps to relax the tension between the supersymmetric contribution to the muon $g-2$ and the one to the Higgs mass. In addition, the broken LR symmetry implies different GUT masses for the soft left- and right-handed matter scalar masses which can be quantified as $m_R \equiv x_{LR} m_L$, where m_R (m_L) denotes the SSB mass of the right-handed (left-handed) fields. As in the previous models, the boundary conditions for the SSB mass terms also involve nonuniversal mass terms for the MSSM Higgs fields.

The values for the input parameters at the GUT level used for the aLR 4-2-2 model described above are

$$\begin{aligned} 0 \leq m_L &\leq 5\,\text{TeV}, \\ 0 \leq M_{2L} &\leq 5\,\text{TeV}, \\ -3 \leq M_3 &\leq 5\,\text{TeV}, \\ -3 \leq A_0/m_L &\leq 3, \\ 1.2 \leq \tan\beta &\leq 60, \\ 0 \leq x_{LR} &\leq 3, \\ -3 \leq y_{LR} &\leq 3, \\ 0 \leq x_d &\leq 3, \\ -1 \leq x_u &\leq 2. \end{aligned} \tag{17}$$

After performing an RGE run as described in the previous section and imposing the constraints in equation (14), our results are displayed in Figures 6, 7, and 8. The figures display models that satisfy EWSB and present a neutralino as the LSP. Figure 6 shows that most of the models tested are excluded due to their low prediction for m_h. However, we find that some of

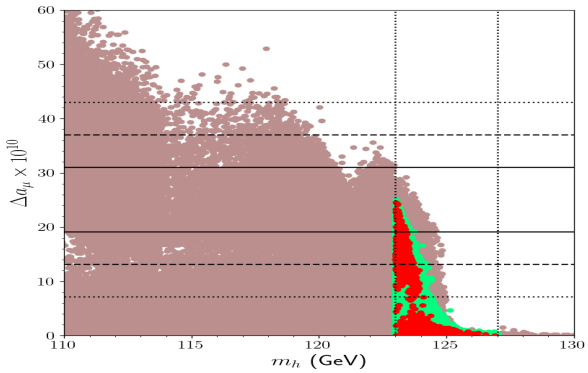

FIGURE 6: The $\Delta a_\mu - m_h$ planes for models obtained in the aLR 4-2-2 scenario. All solutions are compatible with the REWSB and LSP neutralino conditions. The green points are allowed by the mass bounds and constraints from rare B-meson decays. The red points form a subset of green and they satisfy the Planck measurements on the relic density of LSP neutralino within 5σ. The horizontal solid, dashed, and dotted lines bound the regions which accommodate the muon $g-2$ resolution within 1σ, 2σ, and 3σ, respectively.

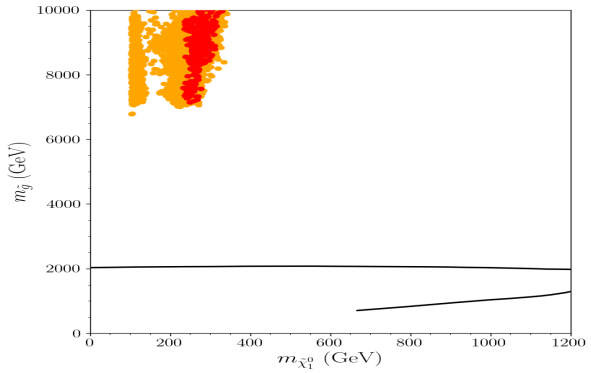

FIGURE 7: Plane $m_{\tilde{g}} - m_\chi$ for the aLR 4-2-2 scenario. The colors represent the same models as in Figure 6 while the solid line represents the area at the reach of the LHC. We denote now in orange the models compatible with the muon $g-2$ measurements within $3-\sigma$.

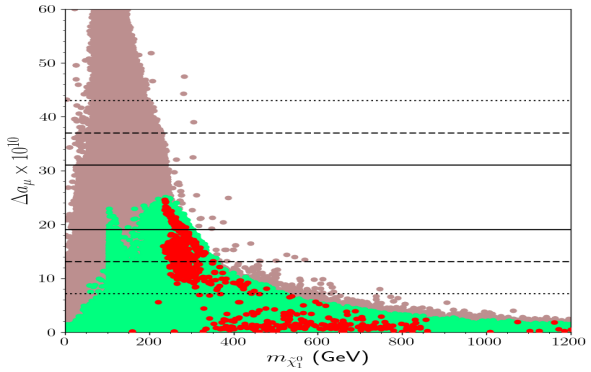

FIGURE 8: Plane $\Delta a_\mu^{\rm SUSY} - m_\chi$ for the aLR 4-2-2 model. The colors represent the same models as in Figure 6.

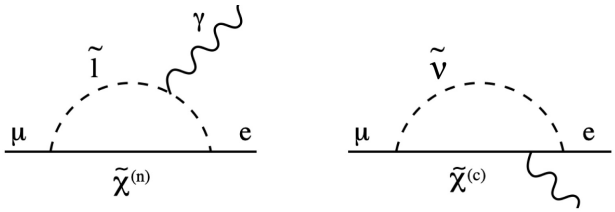

FIGURE 9: Generic Feynman diagrams for $\mu \to e\gamma$ decay: $\tilde{l}$ represents a charged slepton (left) or sneutrino (right), and $\tilde{\chi}^{(n)}$ and $\tilde{\chi}^{(c)}$ represent neutralinos and charginos, respectively.

the points that satisfy the constraints in equation (14) can also explain the muon $g-2$ within $1-\sigma$. Moreover, we find also many models (red dots) that can satisfy the Planck bounds on the relic density of LSP neutralino within $5-\sigma$.

It is interesting to compare the values of the gluino masses for the aLR 4-2-2 model in Figure 7 with the predictions of the $SO(10)$ and sLR 4-2-2 of Figures 4 and 5 from the previous section. In the aLR 4-2-2 framework, the new GUT relations for the gaugino masses push M_3 to large values. Hence, this allows increasing the splitting between squark and selpton masses. Therefore, it is possible to have interesting values for $\Delta a_\mu^{\rm SUSY}$ while keeping m_h inside the experimental bounds. Consequently, the values shown in Figure 8 are larger than the ones of the models of the previous section. Despite the fact that we find models with relevant values for $\Delta a_\mu^{\rm SUSY}$ in the three frameworks, the aLR 4-2-2 case is the only one that can solve the muon $g-2$ problem within $1-\sigma$.

5. MUON $g-2$ AND LEPTON-FLAVOR MIXING EFFECTS

The SM does not predict flavor violation in the leptonic sector. Therefore, the observation of neutrino flavor oscillations has been considered a solid manifestation of Physics Beyond the SM. However, the phenomena that violate flavor have not been yet observed in charged leptons (cLFV). SUSY theories can predict some of these phenomena such as the LFV decays $l_j \to l_i\gamma$, where l_i and l_j are charged leptons with different flavors [41, 42]. Figure 9 shows that the interaction and particles that mediate these decays are similar to the ones that contribute to the muon $g-2$ shown in Figure 1. Therefore, it is interesting to investigate whether the models that can solve the muon $g-2$ problem can also provide interesting predictions for cLFV processes.

The models presented in the previous section assume flavor universal soft terms, and thus, they do not include other sources of flavor violation in addition to the ones of the SM. However, the explanation of observed neutrino flavor oscillations [43, 44, 45, 46] requires an extension of this framework. In

a forthcoming work, we will discuss in detail some of the possible scenarios [47]; here, we just present some results using the general type I seesaw discussed in [23, 29].

In the seesaw scenarios, experimental data can be fitted by extending the MSSM with renormalizable interactions. We consider type I seesaw, in which neutrino masses of the order of 0.1 eV can be obtained by introducing additional singlet RH neutrino at the 10^{13} GeV scale. This mechanism can appear naturally in GUTs without affecting the running of the gauge couplings and, therefore, their unification.

In the 4-2-2 GUT, the breaking of the $SU(2)_R$ symmetry can lead to different seesaw scenarios, in particular type I.[1] Here, we assume that the breaking of the GUT symmetry results in MSSM superpotential, supplemented with a type I seesaw:

$$W = W_{\rm MSSM} + Y_\nu^{ij}\epsilon_{\alpha\beta}H_2^\alpha N_i^c L_j^\beta + \frac{1}{2}M_N^{ij}N_i^c N_j^c, \tag{18}$$

where $W_{\rm MSSM}$ is the MSSM superpotential and N_i^c are additional superfields that contain the three singlet (right-handed) neutrinos, ν_{Ri}, and their scalar partners, $\tilde{\nu}_{Ri}$, and M_N^{ij} denote the 3×3 Majorana mass matrix for the heavy right-handed neutrinos. The full set of soft SUSY-breaking terms is given by

$$\begin{aligned} -L_{\rm soft,SI} = &-L_{\rm soft} + \left(m_{\tilde{\nu}}^2\right)_j^i \tilde{\nu}_{Ri}^*\tilde{\nu}_R^j \\ &+ \left(\frac{1}{2}B_\nu^{ij}M_N^{ij}\tilde{\nu}_{Ri}^*\tilde{\nu}_{Rj}^* + A_\nu^{ij}h_2\tilde{\nu}_{Ri}^*\tilde{l}_{Lj} + \text{h.c.}\right), \end{aligned} \tag{19}$$

where $L_{\rm soft}$ contains the MSSM soft SUSY-breaking masses, and $(m_{\tilde{\nu}}^2)_{j'}^i$, A_ν^{ij}, and B_ν^{ij} are the new soft SUSY-breaking parameters in the seesaw sector.

The seesaw mechanism yields three heavy neutral mass eigenstates that decouple at a high energy scale that we denote as M_N. Below this scale, the effective theory contains the MSSM plus a higher-dimensional operator that provides masses for the light neutrinos:

$$W = W_{\rm MSSM} + \frac{1}{2}\left(Y_\nu L H_2\right)^T M_N^{-1}\left(Y_\nu L H_2\right). \tag{20}$$

Although the predictions of the MSSM are not altered by the additional operator, the running of the slepton masses from $M_{\rm GUT}$ to M_N is affected by the Dirac neutrino Yukawa coupling matrix Y_ν that can be of the same order as the fermion Yukawa couplings and therefore induce flavor changing terms on the slepton masses such that they cannot be diagonalized on the same basis as the lepton Yukawa Y_l. For instance, in such a basis and in the leading-log approximation [20], the slepton masses take the following form:

$$\begin{aligned} \left(m_{\tilde{L}}^2\right)_{ij} &\sim \frac{1}{16\pi^2}\left(6m_0^2 + 2A_0^2\right)\left({Y_\nu}^\dagger Y_\nu\right)_{ij}\log\left(\frac{M_{\rm GUT}}{M_R}\right), \\ \left(m_{\tilde{e}}^2\right)_{ij} &\sim 0, \\ (A_l)_{ij} &\sim \frac{3}{8\pi^2}A_0 Y_{l_i}\left({Y_\nu}^\dagger Y_\nu\right)_{ij}\log\left(\frac{M_{\rm GUT}}{M_R}\right), \end{aligned} \tag{21}$$

leading to the prediction of LFV-charged lepton decays at one loop through diagrams like the ones in Figure 9.

In [29, 30], we evaluated the predictions for LFV for several GUT models; here, we follow the same procedure to specify the seesaw parameters, namely, the RH neutrino mass matrix and the product $Y_\nu^\dagger Y_\nu$. As in [29], we use a simple but representative scenario by considering a common RH neutrino mass for the three species, M_N. Then, using the parametrization of Y_ν given in [23, 29], we find

$$Y_\nu^\dagger Y_\nu = \frac{2}{v_u^2}M_R U m_\nu^\delta U^\dagger, \tag{22}$$

where m_ν^δ denote the diagonalized heavy and light Majorana neutrino mass matrices, and the matrix U can be identified with the Pontecorvo-Maki-Nakagawa-Sakata (PMNS) matrix.

The results presented in [29, 30] compare the LFV predictions from several GUT theories with the LHC searches. However, the considered models on these frameworks cannot provide a significant contribution to the muon $g-2$. In this section, we use the aLR 4-2-2 models presented in the previous section. In this framework, it is possible to select a class of models that satisfy the phenomenological constraints listed in equation (14) and, in addition, solve the muon $g-2$ problem.

To compute the LFV BRs, in addition to the selection of parameter of equation (17), we must provide the ones related to the seesaw. This can be achieved by using some values for neutrino masses compatible with the observed neutrino oscillations and a suitable scale for M_N. The choice of $m_\nu^\delta = \text{Diag}(1.1\cdot 10^{-3}, 8\cdot 10^{-3}, 5\cdot 10^{-2})$ eV combined with the value $M_N = 2.5\times 10^{12}$ GeV leads to values for the BR($\mu\to e\gamma$) of the order of the current or projected experimental bounds for SUSY models that can be tested at the LHC.

We find that the values of BR($\tau\to\mu\gamma$) in the type I seesaw framework under consideration are one order of magnitude below the BR($\mu\to e\gamma$) ones, while the experimental bounds are five orders of magnitude apart. Keeping this in mind, we can present our LFV results using the $\mu\to e\gamma$ decay as a reference. Figure 10 shows the prediction for BR($\mu\to e\gamma$) for models obtained in a parameter scan similar to the one presented in the previous section. Here, we select models that predict $\Delta a_\mu^{\rm SUSY}$ within $3-\sigma$ in addition to satisfying the constraints listed in equation (14). All the points on the figure predict neutralinos with a relic density below the $5-\sigma$ upper limit of WMAP in equation (12). The ones marked in green are also above the lower bound and therefore can explain the DM composition. We can also observe that the large variety of coannihilation models presented by the sLR 4-2-2 models of Section 3 is reduced to three: $\tilde{\tau}-\chi$ (orange +), $\tilde{\tau}-\tilde{\nu}-\chi$ (red $\times$), and $\chi^\pm-\chi$ (black +). In addition, we found some models where coannihilations with the NLSP (gray +) are not needed to satisfy the WMAP bounds. The points with BR($\mu\to e\gamma$) above 10^{12} correspond to models with $\chi^\pm-\chi$ coannihilations.

[1] For a review, see [48] and references therein.

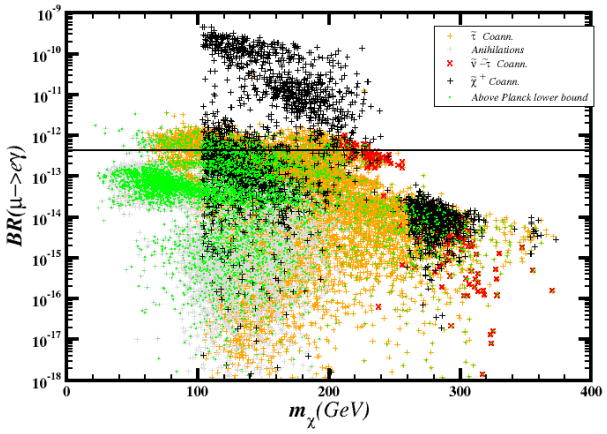

FIGURE 10: Prediction for BR($\mu \to e\gamma$) versus m_χ for ALR 4-2-2 models. All the points are consistent with the upper DM limit and can explain the muon $(g-2)$ within the $3-\sigma$ bound. The green points are the subset of points that predict DM relic density inside the WMAP bounds at the $5-\sigma$ level. The different DM types of models are marked as: grey $\times$ (neutralino annihilations), orange + ($\tilde{\tau}-\chi$ coannihilations), red $\times$ ($\tilde{\tau}-\tilde{\nu}-\chi$ coannihilations and black + ($\chi^{\pm}-\chi$ coannihilations).

These models predict neutralino with a large wino component that cannot account as the only DM component but it can explain the large contribution to $\Delta a_\mu^{\rm SUSY}$. In contrast, we find many models that can explain DM and yet predict values for BR($\mu \to e\gamma$) that can be explored in current experiments [18].

Therefore, we can conclude this section by emphasizing that the SUSY contribution to the muon $g-2$ from the diagrams shown in Figure 1 is not necessarily correlated with a violation of BR($\mu \to e\gamma$) although they involve the same masses and interactions displayed in the diagrams of Figure 9. Furthermore, the MSSM resulting from the aLR 4-2-2 model supplemented with a type I seesaw can explain both DM and muon $g-2$ without entering in contradiction with the current bounds on LFV.

6. CONCLUSIONS

The SUSY extension of the SM can explain the recent experimental values of the muon $g-2$ while predicting DM relic density of cosmological interest. This requires a combination of SUSY masses that may be fitted into a GUT, and therefore, provide a signal of the symmetry group that unifies the SM interactions. We presented the results from several GUT scenarios confronting three models with gaugino unification, such as $SO(10)$, with models where it can be relaxed, such as 4-2-2 models. Regarding the latter, we explored models that preserve a symmetry between left and right fields (sLR 4-2-2) or violate it (aLR 4-2-2).

The three unification groups mentioned above lead to different relations among SUSY masses, and therefore, they present different predictions for phenomena beyond the SM. Indeed, LSP composition is different in each scheme allowing for classification of the models based on the different characteristics of the LSP that can satisfy WMAP bounds. We observed that the class of models with $\tilde{\tau}-\chi$ coannihilations enhance the SUSY contribution to the muon $g-2$; this seems to favor 4-2-2 models over $SO(10)$. Furthermore, between the two realizations of the 4-2-2 studied, the one breaking the LR allows a larger contribution. This is possible because the aLR 4-2-2 framework allows simultaneously relatively light binos and winos that enhance $\Delta a_\mu^{\rm SUSY}$ and heavy gluinos that contribute to keeping m_h inside the experimental bound. Therefore, the tension between both predictions is relaxed.

Regarding LFV, we considered one of the simplest seesaw mechanisms to complement the models such that they can explain neutrino flavor oscillations.[2] In this context, we found that models solving the muon $g-2$ problem can be confronted with the observation of $\mu \to e\gamma$. Despite the fact that the contribution to both processes involve similar SUSY parameters, the relatively low SUSY masses required to explain the muon $g-2$ do not imply a large LFV. Furthermore, many models on aLR 4-2-2 framework can both explain muon $g-2$ and provide good prospects for the $\mu \to e\gamma$ in current experiments.

CONFLICTS OF INTEREST

The authors declare that there are no conflicts of interest regarding the publication of this paper.

ACKNOWLEDGMENTS

This work is supported in part by the United States Department of Energy grant DE-SC0013880 (Q. Shafi and A. Tiwari). The research of M. E. Gómez and C. Salih Ün is supported in part by the Spanish MICINN, under grant PID2019-107844GB-C22. C. Salih Ün also acknowledges the support in part by the Scientific and Technological Research Council of Turkey (TUBITAK) Grant no. MFAG-118F090.

References

[1] E. Komatsu et al. [WMAP Collaboration], "Seven-Year Wilkinson Microwave Anisotropy Probe (WMAP) Observations: Cosmological Interpretation," Astrophys. J. Suppl. **192** (2011) 18 [arXiv:1001.4538 [astro-ph.CO]].

[2] C. L. Bennett et al. [WMAP Collaboration], "Nine-Year Wilkinson Microwave Anisotropy Probe (WMAP) Obser-

[2]The LFV problem with other mechanisms to explain neutrino flavor oscillations is being under current investigation [47].

vations: Final Maps and Results," Astrophys. J. Suppl. **208** (2013) 20 [arXiv:1212.5225 [astro-ph.CO]].

[3] P. A. R. Ade et al. [Planck Collaboration], "Planck 2013 results. XVI. Cosmological parameters," Astron. Astrophys. **571** (2014) A16 [arXiv:1303.5076 [astro-ph.CO]],

[4] P. A. R. Ade et al. [Planck Collaboration], "Planck 2015 results. XIII. Cosmological parameters," Astron. Astrophys. **594** (2016) A13 [arXiv:1502.01589 [astro-ph.CO]].

[5] H. E. Haber and G. L. Kane, "The Search for Supersymmetry: Probing Physics Beyond the Standard Model," Phys. Rept. **117** (1985), 75–263 doi:10.1016/0370-1573(85)90051-1

[6] H. Georgi in "Particles and Fields" 1974, edited by C. E. Carlson, AIP Conference 34 Proceedings No. 23, p. 575.

[7] H. Fritzsch and P.Minkowski, Annals Phys. 93 (1975) 193.

[8] J. C. Pati and A. Salam, "Lepton Number As The Fourth Color," Phys. Rev. D **10**, 275 (1974).

[9] F. Borzumati and A. Masiero, "Large Muon and electron Number Violations in Supergravity Theories," Phys. Rev. Lett. **57** (1986), 961 doi:10.1103/PhysRevLett.57.961

[10] J. A. Grifols and A. Mendez, "Constraints on Supersymmetric Particle Masses From $(g-2)$ μ," Phys. Rev. D **26** (1982), 1809 doi:10.1103/PhysRevD.26.1809

[11] R. Barbieri and L. Maiani, "The Muon Anomalous Magnetic Moment in Broken Supersymmetric Theories," Phys. Lett. B **117** (1982), 203–207 doi:10.1016/0370-2693(82)90547-0

[12] J. R. Ellis, J. S. Hagelin, and D. V. Nanopoulos, Phys. Lett. B **116** (1982), 283–286 doi:10.1016/0370-2693(82)90343-4

[13] B. Abi et al. [Muon $g-2$], "Measurement of the Positive Muon Anomalous Magnetic Moment to 0.46 ppm," Phys. Rev. Lett. **126** (2021) no.14, 141801 doi:10.1103/PhysRevLett.126.141801 [arXiv:2104.03281 [hep-ex]].

[14] G. W. Bennett et al. [Muon $g-2$], "Final Report of the Muon E821 Anomalous Magnetic Moment Measurement at BNL," Phys. Rev. D **73** (2006), 072003 doi:10.1103/PhysRevD.73.072003 [arXiv:hep-ex/0602035 [hep-ex]].

[15] M. Davier, A. Hoecker, B. Malaescu, and Z. Zhang, "Reevaluation of the hadronic vacuum polarisation contributions to the Standard Model predictions of the muon $g-2$ and $\alpha(m_Z^2)$ using newest hadronic cross-section data," Eur. Phys. J. C **77** (2017) no.12, 827 doi:10.1140/epjc/s10052-017-5161-6 [arXiv:1706.09436 [hep-ph]].

[16] K. Hagiwara, R. Liao, A. D. Martin, D. Nomura, and T. Teubner, "$(g-2)_\mu$ and $\alpha(M_Z^2)$ re-evaluated using new precise data," J. Phys. G **38** (2011), 085003 doi:10.1088/0954-3899/38/8/085003 [arXiv:1105.3149 [hep-ph]].

[17] S. Borsanyi, Z. Fodor, J. N. Guenther, C. Hoelbling, S. D. Katz, L. Lellouch, T. Lippert, K. Miura, L. Parato, and K. K. Szabo et al. "Leading hadronic contribution to the muon magnetic moment from lattice QCD," Nature **593** (2021) no.7857, 51–55 doi:10.1038/s41586-021-03418-1 [arXiv:2002.12347 [hep-lat]].

[18] A. M. Baldini et al. [MEG], "Search for the lepton flavour violating decay $\mu^+ \to e^+\gamma$ with the full dataset of the MEG experiment," Eur. Phys. J. C **76** (2016) no.8, 434 doi:10.1140/epjc/s10052-016-4271-x [arXiv:1605.05081 [hep-ex]].

[19] P.A. Zyla et al. [Particle Data Group], "Review of Particle Physics," PTEP **2020** (2020) no.8, 083C01 doi:10.1093/ptep/ptaa104

[20] J. Hisano, T. Moroi, K. Tobe, and M. Yamaguchi, "Lepton flavor violation via right-handed neutrino Yukawa couplings in supersymmetric standard model," Phys. Rev. D **53** (1996), 2442–2459 doi:10.1103/PhysRevD.53.2442 [arXiv:hep-ph/9510309 [hep-ph]].

[21] M. Gómez, G. Leontaris, S. Lola, and J. Vergados, *Phys. Rev.* **D 59** (1999) 116009 [arXiv:hep-ph/9810291].

[22] J. Ellis, M. E. Gómez, G. Leontaris, S. Lola, and D. Nanopoulos, *Eur. Phys. J.* **C 14** (2000) 319 [arXiv:hep-ph/9911459].

[23] J. Casas and A. Ibarra, *Nucl. Phys.* **B 618** (2001) 171 [arXiv:hep-ph/0103065].

[24] S. Antusch, E. Arganda, M. Herrero, and A. Teixeira, *JHEP* **0611** (2006) 090 [arXiv:hep-ph/0607263].

[25] J. Ellis, M. Gómez, and S. Lola, *JHEP* **0707** (2007) 052 [arXiv:hep-ph/0612292].

[26] D. F. Carvalho, J. R. Ellis, M. E. Gomez, and S. Lola, "Charged lepton flavor violation in the CMSSM in view of the muon anomalous magnetic moment," Phys. Lett. B **515** (2001), 323–332 doi:10.1016/S0370-2693(01)00835-8 [arXiv:hep-ph/0103256 [hep-ph]].

[27] M. E. Gomez, Q. Shafi, A. Tiwari, and C. S. Un, "Muon $g-2$, neutralino dark matter and stau NLSP," Eur. Phys. J. C **82** (2022) no.6, 561 doi:10.1140/epjc/s10052-022-10507-6 [arXiv:2202.06419 [hep-ph]].

[28] M. E. Gomez, S. Lola, R. Ruiz de Austri, and Q. Shafi, "Confronting SUSY GUT with Dark Matter, Sparticle Spectroscopy and Muon $(g-2)$," Front. in Phys. **6** (2018), 127 doi:10.3389/fphy.2018.00127 [arXiv:1806.11152 [hep-ph]].

[29] J. Ellis, M. E. Gomez, S. Lola, R. Ruiz de Austri, and Q. Shafi, "Confronting Grand Unification with Lepton Flavour Violation, Dark Matter and LHC Data," JHEP **09** (2020), 197 doi:10.1007/JHEP09(2020)197 [arXiv:2002.11057 [hep-ph]].

[30] M. E. Gómez and S. Lola, "LFV, Dark Matter and LHC Data in Different GUTs," doi:10.31526/ACP.BSM-2021.24

[31] H. Fargnoli, C. Gnendiger, S. Paßehr, D. Stöckinger, and H. Stöckinger-Kim, "Two-loop corrections to the muon magnetic moment from fermion/sfermion loops

in the MSSM: detailed results," JHEP **02** (2014), 070 doi:10.1007/JHEP02(2014)070 [arXiv:1311.1775 [hep-ph]].

[32] M. Carena, S. Gori, I. Low, N. R. Shah, and C. E. M. Wagner, "Vacuum Stability and Higgs Diphoton Decays in the MSSM," JHEP **02** (2013), 114 doi:10.1007/JHEP02(2013)114 [arXiv:1211.6136 [hep-ph]].

[33] K. S. Babu, X. G. He, and E. Ma, "New Supersymmetric Left-Right Gauge Model: Higgs Boson Structure and Neutral Current Analysis," Phys. Rev. D **36** (1987), 878 doi:10.1103/PhysRevD.36.878

[34] T. W. B. Kibble, G. Lazarides, and Q. Shafi, "Walls Bounded by Strings," Phys. Rev. D **26** (1982), 435 doi:10.1103/PhysRevD.26.435

[35] G. Lazarides and Q. Shafi, "Superconducting Membranes," Phys. Lett. B **159** (1985), 261–264 doi:10.1016/0370-2693(85)90246-1

[36] https:twiki.cern.ch/twiki/bin/view/AtlasPublic /SupersymmetryPublicResults https://twiki.cern.ch/twiki/bin/view/AtlasPublic /SupersymmetryPublicResults.

[37] K. S. Babu, B. Bajc, and S. Saad, "Yukawa Sector of Minimal $SO(10)$ Unification," JHEP **02** (2017), 136 doi:10.1007/JHEP02(2017)136 [arXiv:1612.04329 [hep-ph]].

[38] N. Okada, S. Raza, and Q. Shafi, "Particle Spectroscopy of Supersymmetric $SU(5)$ in Light of 125 GeV Higgs and Muon $g-2$ Data," Phys. Rev. D **90** (2014) no.1, 015020 doi:10.1103/PhysRevD.90.015020 [arXiv:1307.0461 [hep-ph]].

[39] M. E. Gómez, Q. Shafi, and C. S. Un, "Testing Yukawa Unification at LHC Run-3 and HL-LHC," JHEP **07** (2020) no.07, 096 doi:10.1007/JHEP07(2020)096 [arXiv:2002.07517 [hep-ph]].

[40] P. Nath, "Supersymmetry unification, naturalness, and discovery prospects at HL-LHC and HE-LHC," Eur. Phys. J. ST **229** (2020) no.21, 3047–3059 doi:10.1140/epjst/e2020-000021-4

[41] L. Calibbi and G. Signorelli, "Charged Lepton Flavour Violation: An Experimental and Theoretical Introduction," Riv. Nuovo Cim. **41** (2018) no.2, 71–174 doi:10.1393/ncr/i2018-10144-0 [arXiv:1709.00294 [hep-ph]].

[42] A. Vicente, "Lepton flavor violation beyond the MSSM," Adv. High Energy Phys. **2015** (2015), 686572 doi:10.1155/2015/686572 [arXiv:1503.08622 [hep-ph]].

[43] S. Fukuda et al. [Super-Kamiokande], "Constraints on neutrino oscillations using 1258 days of Super-Kamiokande solar neutrino data," Phys. Rev. Lett. **86** (2001), 5656–5660 doi:10.1103/PhysRevLett.86.5656 [arXiv:hep-ex/0103033 [hep-ex]].

[44] M. Ambrosio et al. [MACRO], "Matter effects in upward going muons and sterile neutrino oscillations," Phys. Lett. B **517** (2001), 59–66 doi:10.1016/S0370-2693(01)00992-3 [arXiv:hep-ex/0106049 [hep-ex]].

[45] Q. R. Ahmad et al. [SNO], "Direct evidence for neutrino flavor transformation from neutral current interactions in the Sudbury Neutrino Observatory," Phys. Rev. Lett. **89** (2002), 011301 doi:10.1103/PhysRevLett.89.011301 [arXiv:nucl-ex/0204008 [nucl-ex]].
[46]

[46] K. Eguchi et al. [KamLAND], "First results from KamLAND: Evidence for reactor anti-neutrino disappearance," Phys. Rev. Lett. **90** (2003), 021802 doi:10.1103/PhysRevLett.90.021802 [arXiv:hep-ex/0212021 [hep-ex]].

[47] M. E. Gomez, S. Lola, Q. Shafi, and C. S. Un, Work in progress.

[48] F. Hartmann, W. Kilian, and K. Schnitter, "Multiple Scales in Pati-Salam Unification Models," JHEP **05** (2014), 064 doi:10.1007/JHEP05(2014)064 [arXiv:1401.7891 [hep-ph]].